

Interacting Particles in Disordered Flashing Ratchets

Jim Chacko ^{*1} and Goutam Tripathy ^{†2}

^{1,2}Institute Of Physics, Sachivalaya Marg, Bhubaneswar - 751005.
India.

May 1, 2021

Abstract

We study the steady state properties of a system of particles interacting via hard core exclusion and moving in a discrete flashing disordered ratchet potential. Quenched disorder is introduced by breaking the periodicity of the ratchet potential through changing shape of the potential across randomly chosen but fixed periods. We show that the effects of quenched disorder can be broadly classified as strong or weak with qualitatively different behaviour of the steady state particle flux as a function of overall particle density. We further show that most of the effects including a density driven nonequilibrium phase transition observed can be understood by constructing an effective asymmetric simple exclusion process (ASEP) with quenched disorder in the hop rates.

Keywords: Flashing Ratchets, Quenched Disorder, Asymmetric Exclusion Process

PACS: 05.40.-a, 05.60.-k, 87.16.Uv

^{*}E-mail: chacko@iopb.res.in

[†]E-mail: goutam@iopb.res.in

1 Introduction

In systems that are in thermal equilibrium, the second law forbids the existence of a net steady current. However, by continuously driving a system out of equilibrium, a net steady state flux can be obtained. *Flashing Ratchets* are an extensively studied class of systems in which a combination of thermal noise, a periodic asymmetric potential and an external forcing which breaks detailed balance, results in a net directional flux [1, 2]. These have become very relevant as models of active directed transport in intracellular processes as they offer a natural mechanism for maintaining global currents in the absence of a global driving field [3, 4]. The ratchet mechanism has found practical applications in areas of controlling particle motion at nano scale [5, 6], from microfluidics to nanoscale machines [7] and controlling motion of magnetic flux quanta in superconductors [8, 9, 10, 11, 12, 13, 14] .

While bulk of the studies on flashing ratchets involve the motion of a *single* particle (or a set of non-interacting ones), it has become apparent that in many situations interactions between the particles are relevant. This has led to many interesting collective effects in models of elastically coupled motors [15, 16, 17, 1, 3, 4] and excluded volume interactions [18, 19, 20, 21, 22, 23, 24, 25, 26, 27, 28, 29]. Of particular interest to the present work is the model of a discrete flashing ratchet considered in [30, 31] in which large scale properties of a system of hard-core particles moving in a ratchet potential defined on a discrete lattice was studied.

Further, it has been realized that structural non-uniformities or bottlenecks result in frozen disorder that can occur in the tracks along which molecular motors move [32]. Hence, it is natural to study the effects of frozen or quenched randomness on the steady state and dynamics of particles moving in flashing ratchets. Theoretical investigations of effects of this type of disorder on single particle motion in ratchets were reported in [33, 34]. In both these studies nontrivial effects of disorder on mobility and diffusion were found.

In this article, we explore the effects of quenched disorder in the ratchet potential on the steady state properties of the system of particles interacting via hard core constraint. We consider the discrete ratchet model (Model I) studied in [30] and introduce disorder by modifying the shape of the potential over randomly chosen but fixed periods thereby breaking the exact periodicity of the ratchet potential. We find surprisingly close analogy of the disordered ratchet system with an asymmetric exclusion process with quenched but random hop rates (DASEP) [35, 36]. We show that the latter indeed serves as an effective model of the former with reasonable quantitative agreements. Although, we have studied a specific ratchet model, the qualitative results are expected to be applicable to a whole class of similar models.

The outline of this article is as follows. In the Section 2, we introduce the model of the discrete flashing ratchet (FR) and discuss construction of the equivalent asymmetric simple exclusion process (ASEP). Next we introduce quenched disorder in the ratchet potential and present our results for the steady state properties of particle flux and density profiles. We show that the results can be understood through the equivalent disordered asymmetric exclusion process (DASEP). We show that broadly, quenched disorder in these systems may be classified as either *weak* or *strong* with qualitatively distinct effects on steady state properties. In the last section, we conclude and indicate possible future directions of study.

2 Hard core particles moving in a discrete Flashing Ratchet (FR)

In a discrete flashing ratchet (FR), the particle moves among a set of discrete states, e.g., on a lattice in real space, under the influence of a potential that flashes between an ON and an OFF state and thermal noise. In the present work, we consider the model introduced in [30] (Model I), in which the ON state potential $V(x)$ is defined on a one dimensional lattice of unit lattice spacing, $x = 0, \pm 1, \pm 2, \dots$. Fig. 1(a) illustrates the sawtooth potential of integer period w , $V(x + w) = V(x)$ and broken reflection symmetry. The analytical form of $V(x)$ over a period w may be written as (sketched in Fig. 1(b))

$$V(x) = \begin{cases} V_0 x/a & (0 \leq x \leq a) \\ V_0 (w - x)/(w - a) & (a \leq x \leq w), \end{cases} \quad (1)$$

where V_0 is the peak value of the sawtooth potential and a is the asymmetry parameter defining the location of the peak (for $a = w/2$, $V(x)$ is symmetric). We consider a finite lattice of L periods, i.e., the total number of lattice sites in the system is wL . We use periodic boundary conditions to eliminate the effects due to the edges.

In the OFF state ($V = 0$), the particles diffuse with rate r to the nearest empty neighbouring site on the left or right with equal probability (thermal diffusion). The parameter r defines the temperature of the thermal noise ($\beta = 1/r$). In the ON state, particle hops between neighbouring sites n and $m = n \pm 1$ satisfy detailed balance condition with Metropolis rates: $P(n \rightarrow m) = r * \min(1, \exp[\beta(V(n) - V(m))])$. The factor r in the definition of this rate ensures that for $V(x) = 0$, the rates reduce to those in the OFF state. This ensures that the thermal noise used in the ON state is the same as in the OFF state. In one *microstep* a randomly chosen particle

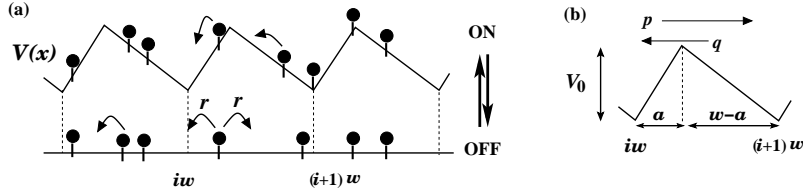


Figure 1: **Fig. 1(a)** is a schematic representation of the particle dynamics on the flashing ratchet. In the ON state, the particles move to neighbouring sites under the influence of $V(x)$ and thermal noise via hopping rates $P(n \rightarrow n \pm 1)$ (see text). In the OFF state, the particles diffuse symmetrically to a neighbouring site with rate r . In both cases, attempted moves are successful only if the target site is empty as a consequence of the hard core constraint. **Fig. 1(b)** is a sketch of the i 'th period of w sites of the sawtooth potential $V(x)$ with the asymmetry parameter a denoting the position of the maximum V_0 . p, q are the effective forward and backward rates of single particle transitions across the i 'th period (see text).

attempts to hop to either of the two neighbouring sites chosen randomly and the transition is completed only if the target site is empty. In a system of N particles (i.e. overall particle density $\rho = N/(wL)$), N such microsteps constitute one Monte Carlo Step (MCS) which serves as the standard unit of time in the model ¹. The flashing ratchet is realized by switching periodically between the ON and OFF states. This switching is independent of the state of the particles and hence it breaks the condition for detailed balance and, together with the asymmetry of $V(x)$, generates a net motion of the particle to the right.

For a frequency ω of flashing, in one period of $1/\omega$ MCS, the ON and OFF states each persist for $1/2\omega$ MCS. The smallest possible period of flashing $V(x)$ is 2 MCS, i.e., the largest possible frequency is $\omega_{max} = 0.5$. In all our simulations reported here we have chosen $r = 1/2$ (i.e., $\beta = 2$), $w = 6$, $V_0 = 5$, $\omega = 0.05$. We have chosen the frequency ω such that the steady state flux is close the maximum possible value (except for Fig. 2(b), in which frequency is varied). For each simulation, the system is initially run for $10^5 - 10^6$ MCS to achieve steady state and then for each data point (steady state flux or density profile) the averaging is done over $10^6 - 10^7$ MCS. In the present study, we switch between the ON and OFF states periodically, we

¹By setting the units of space and time to unity, quantities such as density, speed, frequency, current/flux are dimensionless numbers.

expect that most of the qualitative results would remain valid for a flashing ratchet with more general distribution of switching time scales.

The steady state particle flux or current J (defined as the mean number of particle hops across any bond in 1 MCS in the steady state) for this system is shown in Fig. 2(a) as a function of the overall particle density ρ for two values of the asymmetry parameter $a = 1, 2$. A similar plot was obtained in [30, 31], apart from an overall sign due to different orientation of $V(x)$. The symmetry of the plot around $\rho = 1/2$ is due to the not so apparent particle-hole symmetry of the dynamics, as was elucidated in [30]. To a very good approximation, the plots are quadratic $J(\rho) = A_0\rho(1-\rho)^2$, with strong resemblance to the current-density plot for the Asymmetric Simple Exclusion Process (ASEP) [29]. Indeed, the main point of this paper is an explicit construction by which the discrete flashing ratchet (FR) is mapped to an effective ASEP. As we will see in the next Section, this construction can be naturally extended to the disordered versions of the ratchet model thereby predicting qualitatively correct results that are in fairly good quantitative agreements with direct numerical simulations of the ratchet model.

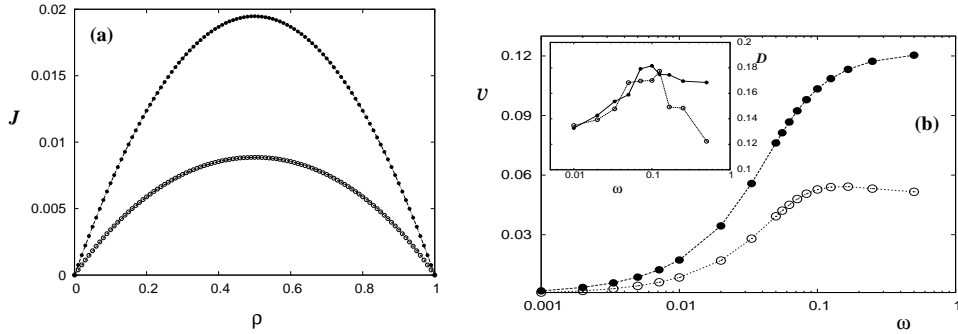


Figure 2: **Fig. 2(a)** is the plot of average particle current J vs overall particle density ρ for the discrete flashing ratchet (FR) for $a = 1$ (filled circles) and 2 (open circles) for $\omega = 0.05$. The plots are approximately of the form $J(\rho) = A_0\rho(1 - \rho)$. **Fig. 2(b)** is the numerically computed mean velocity v and diffusion coefficient D (inset) for a single particle as a function of frequency ω of flashing in the FR for $a = 1$ (filled circles) and $a = 2$ (open circles).

²The most accurate fit to the plots of Fig. 2(a) is of the form $J(\rho) = A_0\rho(1 - \rho) + A_1\rho^2(1 - \rho)^2$ with $(A_0, A_1) = (0.0762, 0.00683)$ and $(0.0393, -0.01530)$ for $a = 1$ and 2 respectively. In fact, up to our numerical accuracy, there are no higher order corrections beyond the A_1 term, which is surprising and needs to be explored further.

Our construction is based on the observation that the coefficient A_0 measured from the $J - \rho$ graph for the interacting ratchet matches with the mean single particle speed v as shown in Fig. 2(b) with other parameters $(V_0, r, a, w, L, \omega)$ remaining the same. This motivates us to propose the equivalent ASEP model as follows: It consists of L sites with the i 'th site of the ASEP corresponding to the i 'th *cell*³ in the FR (as shown in Figs. 3(a)(i), 3(b)(i)). The number of particles in the ASEP equals $L\rho$, keeping the overall particle densities the same as in the original FR model. The following two prescriptions form the core of this construction. (i) The transition rates across the bond $(i, i + 1)$ in the equivalent ASEP, namely, $P(i \rightarrow i + 1)$ and $P(i + 1 \rightarrow i)$ are equal to the effective single particle transition rates p and q respectively between the two cells i and $i + 1$ in the FR (Fig. 1(b)); and (ii) The rates p and q themselves depend upon the potential structure only between the minima of the two adjacent cells $(i, i + 1)$ involved, i.e., the i 'th period. Assumption (ii) implies that p and q are unequal for the FR as the potential structure encountered in the forward (p) and backward (q) transitions are different on account of the asymmetry of $V(x)$. Although, both the above assumptions are strictly true at the single particle level, and the usefulness of this construction is validated by surprisingly close agreement between predictions based on the equivalent ASEP model and direct numerical simulations of the pure as well as disordered ratchet models. The rates p and q are in principle computable from the parameters of the FR [37, 38], however, we compute them from the numerically determined single particle velocity v and diffusion constant D (Fig. 2(b)) using the relations $v = p - q$ and $D = (p + q)/2$ valid for a biased random walker. We adopt this computationally easier approach for the purpose of studying the disordered systems phenomenologically. For the two pure systems of Fig. 2(a), which we name as FR1 ($a = 1$) and FR2 ($a = 2$), the numerical values of v and D are, respectively, $(v_1 = 0.076 \pm 0.001, D_1 = 0.15 \pm 0.01)$ and $(v_2 = 0.039 \pm 0.001, D_2 = 0.15 \pm 0.01)$. As we will see in the next two sections, with the disordered system being constructed from mixing these two pure systems, using these values in the effective models leads to fairly good quantitative agreements.

3 Disordered (discrete) Flashing ratchet (DFR)

We introduce quenched disorder in the flashing ratchet by breaking the periodicity of $V(x)$ through changing the asymmetry i.e. position of the peak a in one or more

³The i 'th cell refers to sites between two maxima containing the minima at $\{iw\}$ whereas the i 'th period is that between the two minima iw and $(i + 1)w$. For a pure system both are equal. In the disordered models, all periods are of equal length w , cells are of unequal sizes. Cell average of density takes one half contribution from the each of the two edge sites of a cell.

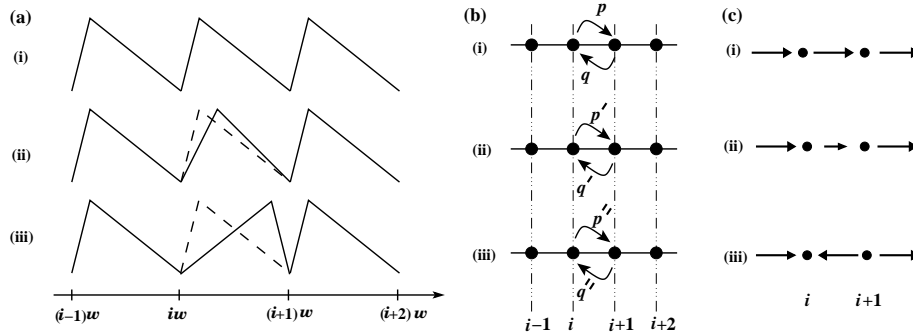


Figure 3: **Fig. 3(a)** is a segment of $V(x)$ shown the (i) pure as well as (ii) *weak* and (iii) *strong* disorder. With weak disorder $a_w = 2$, the position of the peak of the sawtooth is changed but the sign of asymmetry remains the same. For the strong disorder, $a_s = 5$, the sawtooth is flipped thus reversing the sign of asymmetry of that period. **Fig. 3(b)** are the asymmetric exclusion models corresponding to ratchet potentials of Fig 3a. Sites $\{i\}$ of the exclusion model corresponds to the minima $\{iw\}$ of the ratchet potential $V(x)$. The effective rates across the bond $(i, i + 1)$ corresponding to the disordered period are different from the rest of the bonds. **Fig. 3(c)** is a schematic depiction of the net bias $p - q$ on each bond of the equivalent exclusion models of Fig. 3b. The direction of the arrows denote the sign of $p - q$ while the length is proportional to $|p - q|$.

periods of $V(x)$ starting from a pure system in which all periods have $a = 1$. Here, we will consider two representative cases of disordered periods: $a_w = 2$ and $a_s = 5$ (Fig. 3(a)). For $a_w = 2$, the peak position is shifted but the sense of asymmetry of the potential is the same as that for $a = 1$. We call this *weak* disorder. For $a_s = 5$, the asymmetry of the period is opposite to that of $a = 1$. We call this *strong* disorder. As we will see in the sections below, the two cases display significant qualitative differences in the steady state properties. In the fully disordered model a finite fraction f of the L periods are changed and are distributed randomly on the lattice. We call this the Disordered Flashing Ratchet (DFR). We also study a model in which all the disordered periods are put consecutively in one stretch, termed as the Fully Segregated Model (FSM) and show that a mean field approximation becomes exact in this case.

3.1 Weakly Disordered (discrete) Flashing Ratchet (wDFR)

In Fig. 4(a), we plot J -vs- ρ for the disordered flashing ratchet (wDFR) for a single realization of disorder with random distribution of two types of periods $a = 1$ and $a_w = 2$ (with $f = 1/2$). Although, we expect the steady state current in the DFR to lie in between the corresponding values for the two pure systems with $f = 0$ or $f = 1$ (also plotted in Fig. 4(a)), what is significant is the appearance of a plateau for a range of densities $|\rho - 1/2| \leq \Delta$ ($\Delta \simeq 0.2$). In this range of densities (we call it regime B), the steady state flux is independent of the density and is the maximum possible flux in the system. We call the remaining two ranges of densities, $|\rho - 1/2| > \Delta$, regime A .

Further, in Fig. 4(b), we plot the density for the wDFR averaged over each cell as a function of the cell index i . Out of the three representative density values, two values $\rho = 0.1, 0.9$ (top and bottom slides in Fig. 4(b)) belong to regime A while the middle slide (corresponding to $\rho = 0.5$) belongs to regime B . As can be seen from the plots, while in regime A there are density inhomogeneities on scale of a few cells, the system is homogeneous on large length scales. By contrast, in regime B , there are macroscopic regions of different densities separated by microscopically sharp transition regions (shocks). This is akin to a nonequilibrium phase transition which occurs as the overall density is varied.

These two most significant features of the wDFR, namely, the shape of the J -vs- ρ plot and large scale density inhomogeneities in steady state density profiles closely resembles that for the disordered asymmetric simple exclusion process (DASEP) [36]. Indeed, in the following we use the equivalent asymmetric exclusion model constructed following the prescription of the last section to show that the steady state results for the wDFR found above can be qualitatively as well as semi-quantitatively explained from the properties of the constituent pure systems.

The equivalent exclusion model for the wDFR is obtained following the prescription of the previous section and is illustrated in Fig. 3(c). A section of the potential with one disordered period between minima at iw and $(i+1)w$ of the FR is shown in Fig. 3(a)(ii). In the corresponding equivalent exclusion model shown in Fig. 3(b)(ii), the forward (p') and backward (q') transition between the corresponding sites i and $i+1$ are related to v_2 and D_2 of the FR2 through $p' = D_2 + \frac{1}{2}v_2$ and $q' = D_2 - \frac{1}{2}v_2$ as explained in the previous section. Using the values (p, q) and (p', q') for bonds in the equivalent model corresponding to FR1 and FR2 periods respectively, in Fig. 4(d), we compare the steady state density profiles (averaged over each cell) for the wDFR and the equivalent DASEP for $\rho = 0.5$. As can be seen from the plot, the locations of the shocks in the wDFR and the equivalent DASEP match exactly. The shape of the microscopic shocks and, more remarkably, the transition region between the

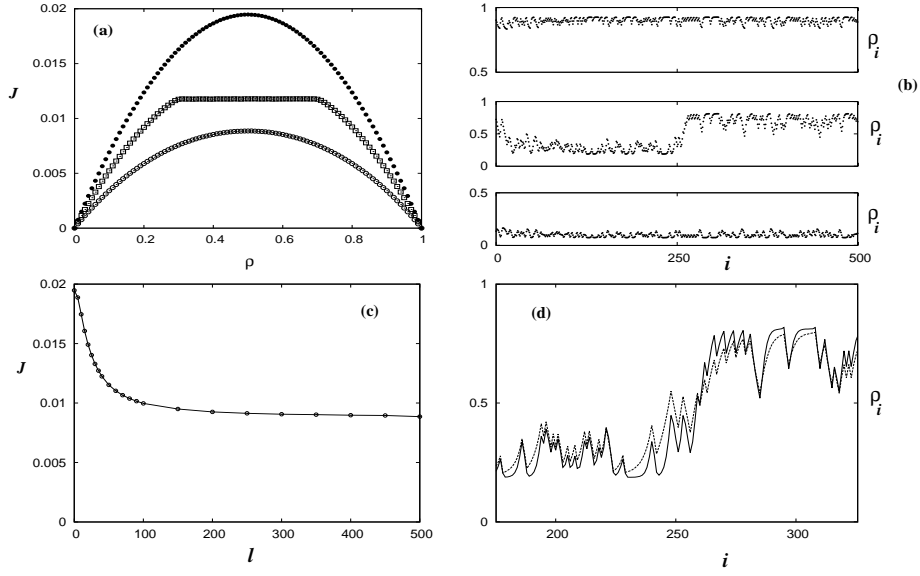


Figure 4: Steady state flux J and density profiles for the wDFR. **Fig. 4(a)** is the plot J -vs- ρ for the weakly disordered flashing ratchet for $L = 500$, $f = 1/2$. The disordered periods are randomly distributed on the lattice. Also shown are the J -vs- ρ for the two corresponding pure systems with $a = 1, 2$. **Fig. 4(b)** are the density profiles $\rho(i)$, averaged over the cell around minima i of $V(x)$, for $\rho = 0.1$ (bottom), 0.5 (middle) and 0.5 (top). **Fig. 4(c)** is the plot of steady state flux J as a function l for a system with a single stretch of disorder of length $l = fL$. **Fig. 4(d)** is the cell-averaged density profile of the wDFR (solid line) for $\rho = 0.5$ (middle box in (b)) compared to the density profile of the equivalent DASEP (dashed line).

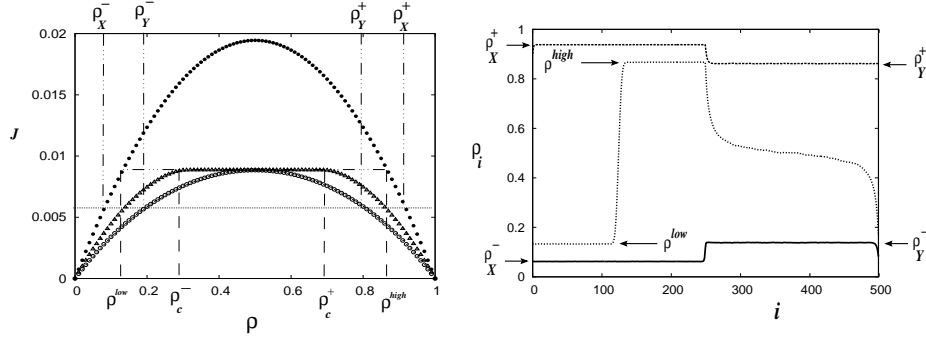


Figure 5: **Fig. 5(a)** is the J -vs- ρ plot for the FSM for the wDFR on a system of $L = 500$. The disordered periods are in a single stretch of $L/2$ periods (i.e. $f = 1/2$). Also shown are the J - vs - ρ of the two corresponding pure systems with $a = 1$ (filled circles), $a = 2$ (open circles). **Fig. 5(b)** is the density profile averaged over each cell for different density of particles, $\rho = 0.1, 0.5, 0.9$. The Y stretch corresponds to $250 < i \leq 500$.

high density and low density phases are captured fairly accurately by the equivalent DASEP.

The plateau in the J -vs- ρ plot (Fig. 4(a)) and the density inhomogeneities (Figs. 4(b), 4(d)) for the wDFR can be qualitatively understood in terms of the equivalent DASEP, as argued in [36]. However, in the following subsection we introduce below the fully segregated model (FSM) which displays similar phenomena as the wDFR and at the same time is amenable to exact analysis.

3.1.1 Fully Segregated Model (FSM)

The Fully Segregated Model (FSM) is obtained from the wDFR by placing the periods with same value of a consecutively together. Let X and Y denote the stretches of periods with $a = 1$ and $a = 2$ respectively. This minimizes the effects due to the small size of the stretches in wDFR. In Fig. 5(a), we plot the J -vs- ρ for the FSM. We see a plateau in the plot that is similar to that in Fig. 4(a) for the wDFR with the quantitative difference that the peak (plateau) current now matches with the peak current for the pure system FR2. In Fig. 5(b), we plot the cell averaged density profiles for the FSM for a density $\rho = 0.5$ in the plateau (regime B) and two densities ($\rho = 0.1, 0.9$) in regime A.

Let ρ_X and ρ_Y denote the steady state densities in the X and Y stretches respectively and J , the steady state current in the system. In regime A , the cell averaged density in each segment is uniform and hence particle conservation implies: $(1-f)\rho_X + f\rho_Y = \rho$ and the equality of the steady state current in both stretches implies: $A_0^X \rho_X(1-\rho_X) = A_0^Y \rho_Y(1-\rho_Y) = J$ (where $A_0^X = v_1$ and $A_0^Y = v_2$). Solving for ρ_Y gives

$$\rho_Y^\pm = \frac{A_0^X f(f+2\rho-1) - A_0^Y(1-f)^2}{2(A_0^X f^2 - A_0^Y(1-f)^2)} \pm \frac{\sqrt{(A_0^X f(f+2\rho-1) - A_0^Y(1-f))^2 + 4A_0^X \rho(\rho+f-1)(A_0^X f^2 - A_0^Y(1-f)^2)}}{2(A_0^X f^2 - A_0^Y(1-f)^2)} \quad (2)$$

$$\rho_X^\pm = \frac{\rho - f\rho_Y^\pm}{1-\rho}, \quad J = A_0^X \rho_X^\pm(1-\rho_X^\pm). \quad (3)$$

As ρ is increased from 0 (decreased from 1), the mean density ρ_X and ρ_Y of each stretch increases (decreases) (Fig. 5(a)). Concurrently, the average current J also increases until the current in the Y stretch reaches its maximum possible value $J_Y^{max} = A_0^Y/4$; at this point, the mean density of particles in the Y stretch is $\rho_Y = 1/2$ (the deviation from a uniform value of $1/2$ is due to the boundaries and this becomes negligible in the limit of large value of Y stretch length $(1-f)L$). This marks the onset of regime B which occurs when the overall particle density reaches the critical value $\rho = \rho_c^-$ (ρ_c^+); where $\rho_c^\pm = \frac{1}{2} \pm \frac{1-f}{2} \sqrt{1 - \frac{A_0^Y}{A_0^X}}$. Thus, the width of the B regime is $2\Delta = (1-f)\sqrt{1 - \frac{A_0^Y}{A_0^X}} = (1-f)\sqrt{1 - v_2/v_1}$. Further increase (decrease) of the density does not affect the density in the Y stretch, rather, the excess (deficit) density is incorporated in the X stretch by the creation of a high (low) density region of density $\rho_X = \rho^{high}(\rho^{low})$. Thus, in regime B , two phases of densities ρ^{high} and ρ^{low} coexist (Fig. 5(b)). The two densities, ρ^{high} and ρ^{low} are related by $\rho^{high} + \rho^{low} = 1$, so that the current in the two phases of the X stretch are equal. For this current to be equal to that in the Y stretch demands $A_0^X \rho^{high}(1-\rho^{high}) = A_0^X \rho^{low}(1-\rho^{low}) = A_0^Y/4$. Thus, $\rho^{high,low} = \frac{1}{2}(1 \pm \sqrt{1 - \frac{A_0^Y}{A_0^X}})$ and the fraction of these phases is given by (using a lever rule) $\phi_X^{low,high} = |\rho - \rho_c^\pm|/(\rho^{high} - \rho^{low})$.

The fact that the system chooses to go in to a state with large scale density inhomogeneity is a consequence of the the extremum current principle that seems to be valid in regime B : If there are more than one apparent choice of steady states, the system would select the one that extremizes the mean current. Such a principle has been shown to be valid in ASEP with open boundaries [39, 40], in disordered ASEP

[36] and has been more recently applied in determining steady states in molecular motor systems [41, 42].

Now, let us try to understand qualitatively the results obtained for the wDFR (Fig. 4) in terms of those of the FSM. The wDFR may be looked upon as obtained from FSM by randomly scrambling the X and Y stretches of the latter. Thereby, the density profiles corresponding to regime A of the wDFR (top and bottom slides in Fig. 4(b)) are similarly scrambled versions of the corresponding density profiles of the FSM (top and bottom graphs in Fig. 5(b)). The microscopic shocks in the former are essentially the alternation between ρ_X^+ and ρ_Y^+ (for $\rho > \rho_c^+$) or between ρ_X^- and ρ_Y^- (for $\rho < \rho_c^-$). As expected, the exact numerical values are slightly different from that of the FSM on account of the smallness of the stretches in the wDFR. Similarly, the phase segregated density profile in regime B of the wDFR (middle slide in Fig. 4(b)), corresponds to an alternation of densities between ρ^{high} and $1/2$ (the *high* density phase) and that between ρ^{low} and $1/2$ (the *low* density phase). Again the actual values of the densities are different on account of the smallness of the stretches in wDFR. Also, density profiles within the same stretch are far from being spatially uniform, unlike that in the FSM, due to strong boundary induced correlation effects.

The J -vs- ρ plot for the wDFR (Fig. 4(a)) is a direct analogue of the same plot for the FSM with the important difference being the high value of the peak (plateau) current in the former. This is in fact a direct consequence of the small lengths of the Y stretches in the wDFR. In Fig. 4(c), we have plotted the peak current of the FSM as a function of the length of the Y stretch. The peak current approaches the peak current of the FR2 beyond a Y stretch length of about $l \simeq 100$. By contrast, the length of the longest Y stretch in the disorder realization of Fig. 4(a) is $l_{max} \simeq 35$. This corresponds to a peak current for the corresponding FSM of 0.012 which is very close to what is observed in Fig.4(a). It should be noted that, in the thermodynamic limit (i.e., $L \rightarrow \infty$), the largest stretch of Y also becomes large ($l_{max} \sim \ln L$) and thus the J -vs- ρ plot for the fully disordered wDFR coincides with that of the FSM (with the same value of f). This feature of nonzero peak current in the thermodynamic limit is what distinguishes wDFR from sDFR. As we will show in the next subsection, in the latter, the steady state current vanishes in the thermodynamic limit $L \rightarrow \infty$.

3.2 Strongly Disordered Flashing Ratchet (sDFR)

A strongly disordered flashing ratchet (sDFR) is obtained if the asymmetry of the disordered period is opposite to that of the other periods. This is achieved by shifting the peak of $V(x)$ to $a_s > w/2$ while the starting model has all periods with $a < w/2$. We chose the sDFR model with a fraction f of periods with $a_s = w - a = 5$ and

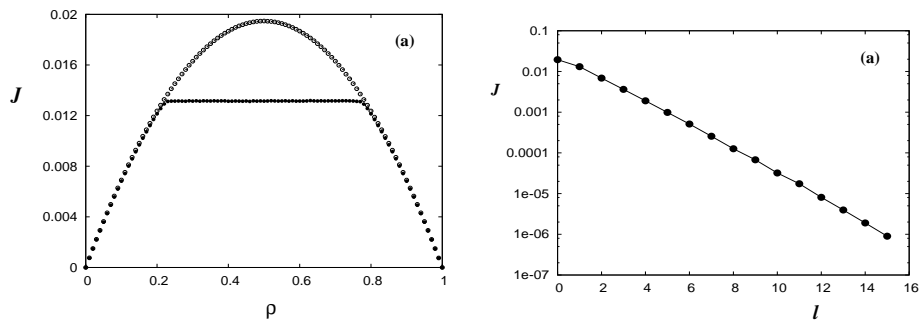


Figure 6: **Fig. 6(a)** is the J -vs- ρ plot for the flashing ratchet with strong disorder with one disorder period $f = 1/L$ for a system of $L = 500$ periods. **Fig. 6(b)** is the steady state flux J for $\rho = 1/2$ with one stretch of $l = fL$ reversed periods. The flux vanishes exponentially with the length of the stretch.

a fraction $1 - f$ of periods with $a = 1$. Clearly, the currents for the two pure systems $f = 0$ and $f = 1$, which are mirror reflections of each other, are related by $J_{w-a} = -J_a$ and therefore for $f = 1/2$, the steady state current in the sDFR vanishes.

In Fig. 6(a), we plot the numerically obtained J -vs- ρ for the sDFR for a single defect period. It is seen the same plateau structure appears here as in the case of the wDFR, however, it should be noted that the reduction in the peak value of the current is significant considering there is only one defect period. As in case of the wDFR, the peak flux is determined by the longest stretch of disorder. Indeed, in Fig. 6(b), we have plotted the peak current as a function of the length $l = fL$ of a single defect stretch (i.e., in the corresponding FSM) for a system of size $L = 500$ and density $\rho = 0.5$. We see that the peak current vanishes exponentially ($J_l \sim e^{-\alpha l}$) with l unlike in the case of wDFR (Fig. 4(c)), where it approaches a finite value. This result has significant implication for the thermodynamic limit of the fully disordered sDFR. In a system of L periods with a finite fraction f of reversed periods, statistically, the length of the longest reversed stretch l_{max} increases a $\ln L$ [43, 36]. Since this longest stretch of reversed periods determines the peak current $J_{max} \sim e^{-\alpha l_{max}}$, thus, for large L the peak current $J_{max} \sim L^{-\alpha}$. I.e., in the thermodynamic limit the flux vanishes for the sDFR. This is in contrast to the single particle result obtained in [33] where the single particle velocity vanishes only in certain ranges of flashing frequency ω .

The results for the sDFR are similar to those for the DASEP with backbends studied in [36]. In fact, using the construction proposed in Section 2, the sDFR translates to a DASEP with local reverse bias in the bonds corresponding to the disordered periods (Fig. 3(c)). The stretches of disordered periods act as backbends and this leads to the vanishing of the particle flux in the thermodynamic limit [43].

4 Results and Discussions

In this article we have studied the effect of quenched disorder in a one dimensional discrete model of the flashing ratchet with hard core particles (motors). We measure the steady state particle flux as density of particles and disorder are varied. We have shown that disorder can be classified broadly as strong or weak depending upon whether the steady state flux vanishes or not in the thermodynamic limit. While in case of weak disorder, the steady state flux has a non zero finite value in this limit, that in case of strong disorder vanishes as a power law of system size.

We further show that, in disordered ratchets, the fundamental diagram (J -vs- ρ plot) has a plateau, i.e., the maximum particle flux is independent of the overall particle density for a range of densities. Inspection of the spatial density profile shows that corresponding to this plateau regime there is large scale spatial segregation of high and low density phases in the disordered system. Through a mapping to an equivalent asymmetric exclusion model using single particle parameters of the ratchet, we show that these features for the disordered interacting ratchets are qualitatively similar as well as quantitatively close to those observed for the disordered asymmetric exclusion process (DASEP).

5 Conclusions

As a test of the basic prescription, proposed in the present report, of extending single particle rates and the assumption that these rates can be locally determined needs to be checked for different forms of disordered ratchets, e.g., by introducing more than two types of periods as has been considered here, or introducing disorder via having periods of different lengths (i.e., disorder in w) and/or in the potential barrier height V_0 in the ON state. Further, effects of disorder in systems with open boundaries is a possible area to explore.

In this paper we have focused our attention on the steady state properties of the systems. The dynamics of fluctuations in the steady state is expected to show interesting behaviour considering the results for the same in the disordered ASEP.

E.g., as noted in [30], in the phase segregated state, the vanishing of the kinematic wave speed may lead to a different dynamic universality class for the fluctuations. This would be an interesting aspect to explore.

References

- [1] P Reimann *Phys. Rep.* **361** 57 (2002)
- [2] S Denisov, S Flach and P Hänggi *Phys. Rep.* **538** 77 (2014)
- [3] F Jülicher, A Adjari and J Prost *Rev. Mod. Phys.* **69** 1269 (1997)
- [4] P C Bressloff and J M Newby *Rev. Mod. Phys.* **85** 135 (2013)
- [5] P Hänggi, F Marchesoni and F Nori *Annalen der Physik* **14** 51 (2005)
- [6] S Savel'ev and F Nori *Chaos* **15** 026112 (2005)
- [7] P Hänggi and F Mascheroni *Rev. of Mod. Phys.* **81** 387 (2009)
- [8] J F Wambaugh, C Reichhardt, C J Olson, F Marchesoni and F Nori *Phys. Rev. Lett.* **83** 5106 (1999)
- [9] J E Villegas, S Savel'ev, F Nori, E M Gonzalez, J V Anguita, R Garca and J L Vicent *Science* **302** 1188 (2003)
- [10] Y Togawa, K Harada, T Akashi, H Kasai, T Matsuda, F Nori, A Maeda and A Tonomura *Phys. Rev. Lett.* **95** 087002 (2005)
- [11] B Y Zhu, F Marchesoni, V V Moshchalkov and F Nori *Phys. Rev. B* **68** 14514 (2003)
- [12] F Nori *Nature Physics* **2** 227 (2006)
- [13] B Y Zhu, F Marchesoni and F Nori *Phys. Rev. Lett.* **92** 180602 (2004)
- [14] S Savel'ev, V Misko, F Marchesoni and F Nori *Phys. Rev. B* **71** 214303 (2005)
- [15] F Jülicher and J Prost *Phys. Rev. Lett.* **75** 2618 (1995)
- [16] E B Stukalin, H Phillips III and A B Kolomeisky, *Phys. Rev. Lett.* **94** 238101 (2005)

- [17] J Bruges and J Casademunt *Phys. Rev. Lett.* **102** 118104 (2009)
- [18] I Derenyi and T Vicsek *Phys. Rev. Lett.* **75** 374 (1995)
- [19] I Derenyi and A Ajdari *Phys. Rev. E* **54** R5 (1996)
- [20] S Savel'ev, F Marchesoni and F. Nori *Phys. Rev. E* **71** 011107 (2005)
- [21] T Tripathi and D Chowdhury *Phys. Rev. E* **77** 011921 (2008)
- [22] D Chaudhuri and A Dhar *Europhys. Lett.* **94** 30006 (2011)
- [23] N Golubeva and A Imparato *Phys. Rev. Lett.* **109** 190602 (2002)
- [24] P Tierno and T M Fischer *Phys. Rev. Lett.* **112** 048302 (2014)
- [25] S Savel'ev, F. Marchesoni and F Nori *Phys. Rev. Lett.* **91** 010601 (2003)
- [26] S Savel'ev, F Marchesoni and F Nori *Phys. Rev. Lett.* **92** 160602 (2004)
- [27] S Savel'ev, F Marchesoni and F Nori *Phys. Rev. E* **70** 061107 (2004)
- [28] S Savel'ev, F Marchesoni, A Taloni and F Nori *Phys. Rev. E* **74** 021119 (2006)
- [29] T Chou, K Mallick and R K P Zia *Rep. Prog. Phys.* **74** 116601 (2011)
- [30] Y Aghababaie, G I Menon and M Plischke *Phys. Rev. E* **59** 257 (1999)
- [31] G I Menon *Physica A* **372** 96 (2006)
- [32] T Chou and G Lakatos *Phys. Rev. Lett.* **93** 198101 (2004)
- [33] T Harms and R Lipowsky *Phys. Rev. Lett.* **79** 2895 (1997)
- [34] F Marchesoni *Phys. Rev. E* **56** 2492 (1997)
- [35] G Tripathy and M Barma *Phys. Rev. Lett.* **78** 3039 (1997)
- [36] G Tripathy and M Barma *Phys. Rev. E* **58** 1911 (1998)
- [37] J A Freund and L Schimansky-Geier *Phys. Rev. E* **60** 1304 (1999)
- [38] J C Latorre, P R Kramer and G A Pavliotis *J. of Comp. Phys.* **257** 57 (2014)
- [39] J Krug *Phys. Rev. Lett.* **67** 1882 (1991)

- [40] V Popkov and G Schtz *Europhys. Lett.* **48** 257 (1999)
- [41] A Basu and D Chowdhury *Phys. Rev. E* **75** 021902 (2007)
- [42] I Pinkoviezky and N S Gov *Phys. Rev. E* **88** 022714 (2013)
- [43] M Barma and R Ramaswamy *Non-linearity And Breakdown in Soft Condensed Matter* (eds) K K Bardhan, B K Chakrabarti and A Hansen (Berlin: Springer-Verlag) p 309 (1993)